

## Diffraction efficiency of transient grating and relaxation profiles of some laser dyes

R Justin Rajesh, Mini Jose and Prem B Bisht\*

Department of Physics, Indian Institute of Technology Madras, Chennai-600 036, India

E-mail : bisht@iitm.ac.in

Received 9 September 2002, accepted 9 October 2002

**Abstract** : Self-diffraction efficiency of laser dyes have been measured and compared with theoretical values for some dyes. Effect of refractive index of the solvent on the diffraction efficiency has also been studied. Degenerate four wave mixing have been used to measure the excited state relaxation profiles to estimate the orientational relaxation times in ps time scale.

**Keywords** : Laser induced transient grating, self-diffraction, degenerate four wave mixing, third order nonlinear susceptibility.

**PACS Nos.** : 42.62.Fi, 42.65.Hw, 42.65.An

### 1. Introduction

Fluorescence of a dye takes place as a result of creation of a short lived entity, the excited state. The optical properties of a molecule are spatially modulated in the interference region of two intense light waves. Laser-induced change of the optical property is caused by the changes involving both, the refractive index and the absorption coefficient. If the wavelength of the pump laser pulse falls under the absorption spectrum of the molecule, then inside the interference pattern, a population density grating is created, the decay of which corresponds to the relaxation mechanism of the excited state. Experimentally, two collimated TEM<sub>00</sub> pulsed laser beams, which are close to an ideal plane wave give rise to the laser induced transient grating (LITG) when brought to intersection [1]. By observing the diffracted light of the grating, it is possible to deduce the non-linear optical properties of the sample [2–5].

The principle of LITG is indicated in Figure 1. The pump pulse is split into two pulses *A* and *B* with wave vectors  $k_A$  and  $k_B$ . The two beams intersect at an angle  $\theta$  at the sample and create an interference pattern with the vector  $q = \pm(k_A - k_B)$ . The remarkable feature is that the beams that produce the grating also get diffracted for thin grating.

This is known as self-diffraction. The first-order self-diffraction of one beam overlaps with the very weak second

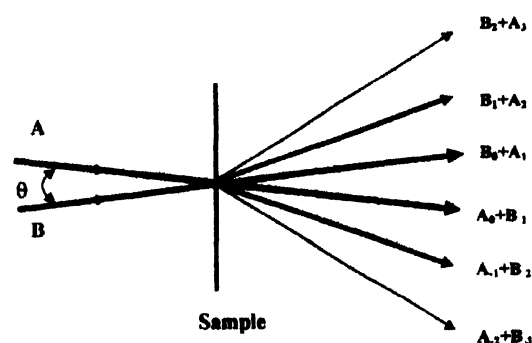


**Figure 1.** Formation of a laser induced transient grating (LITG) as a result of interference of two pulses (*A* and *B*). Subscripts 0, 1, 2, denote the order of the diffraction  $\theta$  is the angle between the pump beams.

order self-diffraction of the other beam [1]. The Bragg condition applies for the diffracted beams from an optically thick grating and the combined interference and diffraction effect therefore corresponds to four-wave mixing. The process is called degenerate if the frequencies of the three incident waves and the generated wave are equal. Dynamic diffraction gratings can be amplitude or phase gratings, and are characterized by changes of the absorption coefficient

\*Corresponding Author

$\Delta K$  and the refractive index  $\Delta n$ , respectively. From the ratio of the incident and diffracted intensities of a beam, the diffraction efficiency ( $\eta$ ) can be calculated [1–5].

Moog *et al* [6] have measured the decay rates of the excited states in rhodamine B (RB) by using transient grating technique in solvents of varying viscosity. Weise *et al* [2] have calculated  $\chi^{(3)}$  of cresyl violet (CV) in methanol by measuring the diffraction efficiency of LITG as a function of the concentration of the dye. Langhans *et al* [3] have measured the diffraction efficiency and the anisotropic decay profiles of decay of LITG for Rhodamine 6G (R6G) in methanol. Vauthey and coworkers [7–9] have extensively studied excited state phenomena by using Bragg geometry of LITG with ps and fs pulsed lasers. Terazima [10] have reviewed the photothermal studies of several excited-state processes by LITG method.

Recently, we reported our preliminary results on theoretical and experimental studies on LITG in N, N'-bis(2,5-di-tert-butylphenyl)-3,4 : 9-10-perylenebis(dicarboximide) (DBPI) [5]. In the present paper, the self-diffraction efficiencies and the third order nonlinear susceptibility ( $\chi^{(3)}$ ) values are given for several dyes *viz.* R6G, Rhodamine B (RB), CV, pyridine 1, IR 140, Eosin, IR 26 along with that of DBPI. The theoretical values of diffraction efficiency have been calculated using Kramer's-Kronig relation. These values have been compared with the experimental values for some of the laser dyes. In addition, the effect of refractive index on the self-diffraction efficiency of transient grating and  $\chi^{(3)}$  have been studied for R6G. The temporal evolution of LITG has been recorded for dyes by diffraction of a third probing pulse derived from the same laser to deduce the relaxation times in the excited state.

## 2. Theory

### 2.1. Diffraction efficiency :

As described in Figure 1, two-beam interference produces a spatially modulated light field, which is called an interference grating. It can be an amplitude or a phase grating characterized by changes of the absorption coefficient ( $\Delta K$ ) or the refractive index ( $\Delta n$ ), respectively. Population density gratings exhibit a mixed amplitude and phase response, dependent on the probe wavelength. Excitation of dynamic gratings is also possible by interfering beams with different polarization.  $\Delta K$  is related to the absorption cross sections of the ground state ( $\sigma_{a0}$ ), the first excited state ( $\sigma_{a1}$ ) and the stimulated emission cross section to the ground state ( $\sigma_{e0}$ ) of the sample by the relation [1–3]

$$\Delta K = \frac{1}{2}(\sigma_{a0} - \sigma_{a1} + \sigma_{e0})N_1. \quad (1)$$

For a thin sample, the number of molecules in the excited state  $N_1$  is given by

$$N_1 = N_0 \left[ 1 - e^{-\frac{\sigma_{a0} W_p}{h\nu}} \right] \quad (2)$$

where  $W_p$  is the total peak energy density of both the excitation pulses.

Diffraction efficiency ( $\eta$ ) of the thin grating is experimentally measured by taking the ratio of the intensity of the diffracted signal ( $I_D$ ) to that of the transmitted intensity ( $I_T$ ) of one of the laser beams producing the grating [1],

$$\eta = I_D / I_T. \quad (3)$$

The efficiency of diffraction of a sample of thickness  $d$  can be calculated theoretically by using  $\Delta K$  and  $\Delta n$  according to the following eq. [1–5]

$$\eta = \frac{9m^2}{25} \frac{d^2}{4} (\Delta K^2 + k^2 \Delta n^2), \quad (4)$$

where  $m = 2(I_1 I_2)^{1/2} / (I_1 + I_2)$  is the visibility of interference fringes [2,3] (here  $I_1$  and  $I_2$  are the intensities of the two pump beams and  $k = 2\pi/\lambda$ , where  $\lambda$  is the vacuum wavelength of the diffracted light wave).  $\Delta n$  at the wavelength ( $\lambda$ ) can be calculated by the following Kramers-Kronig relation [11]

$$\Delta n(\lambda) = \frac{N_1}{\pi^2} \int \frac{\sigma_{a1}(\lambda') - \sigma_{e0}(\lambda') - \sigma_{a0}(\lambda')}{1 - (\lambda'/\lambda)^2} d\lambda'. \quad (5)$$

The square of the absolute value of the third-order nonlinear susceptibility is related to the efficiency of first order self diffraction by the relation [2]

$$|\chi^{(3)}|^2 = \eta \frac{100n^4 \tau_p^2}{9m^2 Z_0^2 W_p^2 k^2 d^2}, \quad (6)$$

where  $n$  is the refractive index of the medium,  $\tau_p$  is the pulse width,  $k$  is the angular wave number and  $Z_0$  is the wave impedance in free space. The efficiency of Bragg-diffraction of a thick grating has been discussed by Kogelnik [12].

### 2.2. Transient behaviour and coherence spike :

Time-dependent investigations of LITG are performed by sending probe pulses with different time delays and measuring the diffracted intensity. The time profiles obtained from the LITG experiments may contain several contributions such as the coherence peak, optical Kerr effect of the solvent (OKE), density phase grating, acoustic grating and relaxation times of the molecule [8,10,13–17].

The observed decay is governed by the following equation (8,14)

$$I_{TG}(t) = \int I_{Pr}(t-t'') \left| \int \chi^{(3)}(t''-t') I_{Pu}(t') dt' \right|^2 dt'' \quad (7)$$

where  $t$  is the time delay between the pump and the probe pulses,  $I_{Pr}$  and  $I_{Pu}$  are the intensities of the probe and the pump pulses, respectively and  $\chi^{(3)}$  is the third-order nonlinear susceptibility tensor of the sample.  $\chi^{(3)}$  depends upon the polarization of the pump and the probe pulses. At low pump energies for fitting the observed decay by eq. (9), we take the form of  $\chi^{(3)}$  as

$$\chi^{(3)} = A_G e^{-4(t/\tau_G)^2 \ln 2} + A_1 e^{-t/\tau_o} \quad (8)$$

where the first term accounts for the coherence spike and the second one is due to excited state relaxation of solute molecules. Here,  $A_G$  and  $A_1$  are the pre-exponential factors of the time constants  $\tau_G$  (Gaussian pulse width) and  $\tau_o$  (orientational relaxation time), respectively.

### 3. Experimental

High purity grade dyes *viz.* R6G (SERVA), RB (SERVA), CV (SERVA), Pyridine 1 (Lambda Physik), IR 140 (Aldrich), Eosin (BDH), IR 26 (Lambda Physik) and DBPI (Aldrich) were used as received. Freshly opened bottles of spectrograde solvents *viz.* water, acetonitrile (ACN), benzene, ethanol (EtOH), 2-methoxyethanol (MeEtOH), ethylene glycol (EG), 1,2-dichloroethane (DCE), Di methyl sulphoxide (DMSO) were used for preparing the samples. The solutions prepared were kept in dark to protect from light, which may cause bleaching. All measurements were carried out at 300 K.

The experimental set-up for creation and detection of the LITG is shown in Figure 2. A mode-locked frequency-doubled Nd : YAG laser (Continuum model YG601) was used in the experiments. The laser pulse (pulse width of

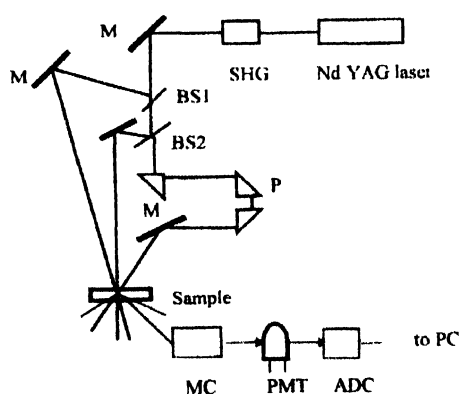


**Figure 2.** Experimental arrangement for measurement of diffraction efficiency of transient grating. SHG : Second Harmonic Generator. M : Mirror, P : Prism, BS1 and BS2 : Beam splitter, MC : Monochromator. PMT : Photomultiplier tube, ADC : Analog-to-digital converter. PC : Personal computer.

35 ps with energy of 0.14 mJ and beam diameter of 5 mm, unless otherwise specified) at 532 nm was split into two pulses by a 30% reflecting beam splitter (BS1). The transmitted beam was further split into two by a 50% beam splitter (BS2). The two reflected pulses from BS1 and BS2 were made to intersect in a liquid sample at an angle of  $5^\circ$  to form the grating. The intensity of one of the first-order self-diffracted beam was measured with the help of a PIN photodiode (Motorola MRD 510) for diffraction efficiency measurement. The transmitted intensity of this beam was measured by reducing the laser intensity by a known factor with the PIN photodiode. The pulse energy was calculated from the average power measured at 10 Hz by a power meter (Ophir 30A-P). The sample was kept in a cell that is made as follows : two thin sheets each of thickness  $0.10 \pm 0.02$  mm were kept separated by a known distance between the two glass plates. Three edges of the glass plates were sealed with an adhesive (Araldite). The thickness of the cell was cross checked by comparing its filled volume with a known volume of a solvent.

For measurement of decay profiles the transmitted beam from BS2 was used as the probe pulse. The probe pulse was sent through the sample in box-type geometry after passing through an optical delay line. The delay line was connected to a computer controlled stepper motor. The Bragg-diffracted probe pulse was made to fall on a photomultiplier tube (RCA 931A) after passing through a monochromator preset at 532 nm to avoid ambient light. The diffracted intensity of the probe was measured as a function of delay of the probe pulse with respect to the excitation pulses. The output of the PMT was sent to a PC through an analog-to-digital converter [18]. The instrument response function was measured by the same set up by using the autocorrelation of 1064 nm pulses at a 2 mm thick L-Arginine phosphate monohydrate (LAP) crystal by sum frequency generation. The PMT output was averaged over twenty shots of the laser pulses before storing in the PC.

Theoretical simulations were done by using standard numerical methods by writing computer program in C language in a UNIX machine [19]. The program was standardized by reproducing the reported values of  $\Delta n$  and diffraction efficiency for R6G and CV [2,3].

### 4. Results and discussion

#### 4.1. Diffraction efficiency and $\chi^{(3)}$ :

Table 1 shows the self-diffraction efficiency values for different dyes in DMSO. The diffraction efficiency and  $\chi^{(3)}$  values were determined experimentally according to eqs. (4) and (6), respectively. The values obtained for R6G are close to those available in literature [2,3]. It can be seen that for a comparable thickness and concentration the dyes R6G, RB, eosin and DBPI are the most efficient for self diffraction

at 532 nm, while IR 140, IR 26 and CV have a low value of diffraction efficiency.

**Table 1.** Diffraction efficiency ( $\eta$ ) and third order susceptibility ( $\chi^{(3)}$ ) of different dyes at 532 nm in DMSO (Total pulse energy = 0.6 m J, Radius of the beam = 4.0 mm).

Dye	$c$ (M)	$l$ (mm)	$\eta$	$\chi^{(3)}$ ( $\text{m}^2/\text{V}^2$ )
R6G	$2.5 \times 10^{-4}$	0.09	$4.42 \times 10^{-4}$	$1.26 \times 10^{-18}$
RB	$5.0 \times 10^{-4}$	0.08	$7.00 \times 10^{-4}$	$1.58 \times 10^{-18}$
CV	$5.0 \times 10^{-4}$	0.12	$0.24 \times 10^{-4}$	$0.29 \times 10^{-18}$
Pyridine 1	$5.0 \times 10^{-4}$	0.17	$2.40 \times 10^{-4}$	$0.93 \times 10^{-18}$
IR 140	$5.0 \times 10^{-4}$	0.06	$0.57 \times 10^{-4}$	$0.46 \times 10^{-18}$
Eosin	$5.0 \times 10^{-4}$	0.08	$7.66 \times 10^{-4}$	$1.66 \times 10^{-18}$
IR 26	$5.0 \times 10^{-4}$	0.08	$1.57 \times 10^{-4}$	$0.75 \times 10^{-18}$
DBPI <sup>(a)</sup>	$2.5 \times 10^{-4}$	0.08	$7.40 \times 10^{-4}$	$1.68 \times 10^{-18}$

<sup>(a)</sup>in benzene.

The absorption cross section in the ground state ( $\sigma_{00}$ ) and the stimulated emission cross section ( $\sigma_{01}$ ) to the ground state were calculated with the help of the measured spectra of dilute solutions of the dyes. The change of the refractive index ( $\Delta n$ ) at a wavelength is calculated by eq. (5). The values of  $\sigma_{00}$  were obtained with the help of optical density (OD) by using the formula  $\sigma_{00} = OD/(N.d)$ , where  $N$  is the number of molecules in the solution. The values of  $\sigma_{01}$  were calculated by using the formula [20]

$$\sigma_{e0}(\lambda) = \frac{\lambda^4 E(\lambda)}{8\pi n^2 c \tau_f} \phi, \quad (9)$$

where  $\tau$  is the fluorescence lifetime,  $c$  is the speed of light,  $\phi$  is the fluorescence quantum yield and  $E(\lambda)$  is the fluorescence intensity profile normalized by the expression  $\int E(\lambda)d\lambda = 1$ . For all calculations, the intensity of excitation beams were taken to be the same. The values of  $\sigma_{01}$  used in the simulations were taken from literature [20].

Figure 3 (panel A) shows a typical simulation for the self-diffraction efficiency for RB in methanol-ethylene glycol

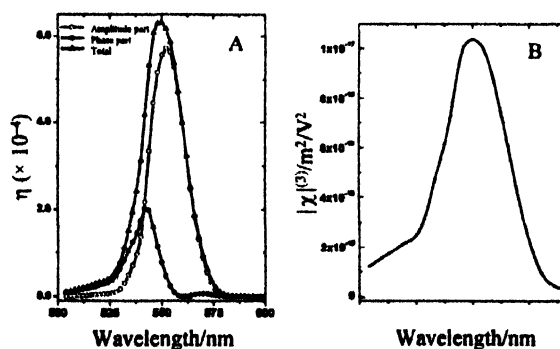


**Figure 3.** Plot of theoretically simulated diffraction efficiency (panel A) and theoretically obtained values of  $|\chi^{(3)}|$  (panel B) as a function of wavelength for RB in methanol-ethylene glycol (1 : 1). The parameters are :  $c = 2 \times 10^{-4}$  M,  $\lambda = 532$  nm and  $\tau_p = 35$  ps,  $W_p = 4 \times 10^{-4}$  J/cm<sup>2</sup> and thickness = 0.05 mm.

mixture (1 : 1). It is seen that the contribution of amplitude grating dominates over the phase grating. Since we are using low energy densities ( $4\sim 7 \times 10^{-4}$  J/cm<sup>2</sup> at 35 ps pulse width), the population grating is free from other effects such as acoustic grating [21]. The efficiency of diffraction is maximum at 550 nm and it vanishes below 500 nm and above 580 nm. This observation indicates that the second harmonic of YAG laser (532 nm) can be used for the self diffraction experiments. The value of diffraction efficiency is close to that obtained experimentally within the errors associated with the parameters of the solvents. Panel B of Figure 3 shows the calculated value of  $\chi^{(3)}$  as a function of the wavelength. For R6G and DBPI the calculated values were found to be in agreement to the experiments [4,5].

The effect of solvent refractive index on the diffraction efficiency and  $\chi^{(3)}$  is indicated in Table 2. The variation

**Table 2.** Effect of refractive index ( $n$ ) on diffraction efficiency ( $\eta$ ) and third order susceptibility ( $\chi^{(3)}$ ). The parameters are :  $d = 0.08$  mm,  $c = 5 \times 10^{-4}$  M

Solvent	$n$	$\eta$	$\chi^{(3)}$ ( $\text{m}^2/\text{V}^2$ )
Water	1.328	$1.21 \times 10^{-4}$	$7.98 \times 10^{-19}$
ACN	1.344	$8.15 \times 10^{-4}$	$2.12 \times 10^{-18}$
EtOH	1.360	$3.40 \times 10^{-4}$	$1.40 \times 10^{-18}$
MeEtOH	1.402	$2.88 \times 10^{-4}$	$1.37 \times 10^{-18}$
EG	1.432	$1.81 \times 10^{-4}$	$1.14 \times 10^{-18}$
DCE	1.443	$4.07 \times 10^{-4}$	$1.73 \times 10^{-18}$
DCE + DMSO (1 : 1)	1.461	$6.11 \times 10^{-4}$	$2.17 \times 10^{-18}$
DMSO	1.479	$4.41 \times 10^{-4}$	$1.89 \times 10^{-18}$

of  $\chi^{(3)}$  as a function of  $n^2$  is shown in Figure 4. By using Lippert's equation [22] for R6G, the change of the dipole moment on excitation has been found to be 2.01 D [23]. This indicates the absence of any specific strong interaction between the fluorophore and the solvent. The plot is linear as is expected from eq. (6) within experimental errors.

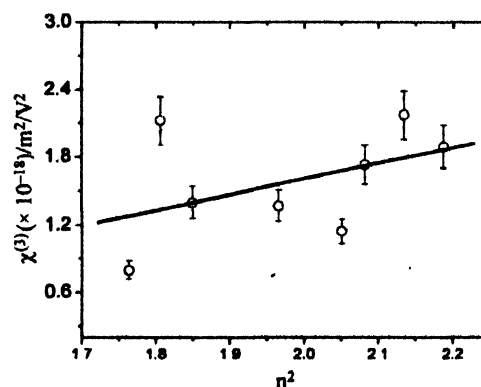


**Figure 4.** Plot of  $|\chi^{(3)}|$  vs  $n^2$  for R6G. The open circles are the data points and the straight line shows the best linear fit (see Table 2). The error bars are within 10%.

#### 4.2. Degenerate four wave mixing and decay profiles :

The box geometry of degenerate four wave mixing was used for measuring the relaxation time by delaying the probe pulse (Figure 5). The decay profiles have been measured with sample thickness of 0.8 mm to increase the diffracted

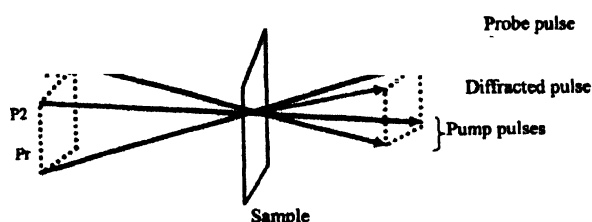


Figure 5. Box geometry used for recording the decay profiles.  $P_1$  and  $P_2$  are the pump pulses while  $P_r$  denotes the probe.

signal. Figure 6 shows the decay profiles of the grating formed by the pump beams at lower pump energy ( $< 0.5$  mJ) for R6G in EG and DBPI in DMSO. The observed decay profiles show a sharp peak at short time followed by decaying components. The decay curves are expressed by eqs. (7) and (8).

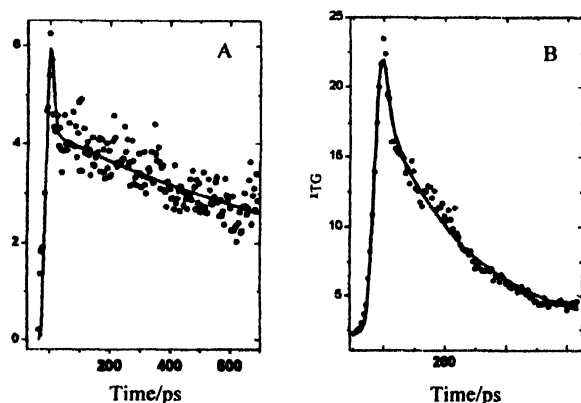


Figure 6. Decay curves (A) for R6G in ethylene glycol and (B) for DBPI in DMSO. Continuous lines show the fitted curve to the data points with eqs. (7) and (8) to give the relaxation times of 2889 ps and 570 ps for data in (A) and (B), respectively.

The sharp peak at zero time is known as the coherence peak that occurs in LITG experiments due to the diffraction of one of the pump beams into the direction of probe diffraction by a grating formed by the other pump beam and the probe beam. The coherence spike appears only when the pump and the probe beams are derived from the same laser [8,14]. A Gaussian profile with a half-width equal to that of the pump laser pulse accounts for this. In any case, the decay curves can have a varying nature depending upon the polarisation of the pump and probe beams, intensity of the incoming beams and wavelength of probe beam. Myers and Hochtrasser [15] have shown this dependence of the decay profiles for R6G in ethylene glycol. In the present case the polarisation of the pump and probe beams is parallel. Since the decay curves are recorded only up to approximately

700 ps, we ignore the fluorescence lifetime component in the analysis that will nearly be a constant. By fitting the limited range of the decay curve with eqs. (7) and (8) the orientational relaxation time ( $\tau_{or}$ ) of the molecule in the solvent can be obtained. The decay curves are obtained after adding 4 curves recorded in a sequence for a sample. Decay profile of R6G in ethylene glycol is given in panel (A) of Figure 6. As can be seen from eq. (8), the analysis requires double deconvolution of the decay curve with the pump pulse. The profile contains a sharp coherence spike followed by a slower decay. Due to only a few points on initial time scale, the data-correlation takes place in the theoretical fitting of experimental data for the parameters associated with the shorter times. However, longer time scale data fit well to give a value of  $2889 \pm 100$  ps for  $\tau_{or}$  which is also reported in the case of RB in ethylene glycol [6]. DBPI in DMSO shows a smaller value of  $570 \pm 30$  ps (panel B). The value of  $\tau_{or}$  is in close agreement to those obtained from Debye-Stokes-Einstein [24] hydrodynamic theory ( $\tau_{or} = \gamma V/k_B T$ , where  $\gamma$  is the viscosity of the solvent,  $V$  is the volume of the molecule and  $T$  is the temperature).

We have found that the dye DBPI is an efficient and stable probe molecule at 532 nm besides RB, R6G and eosin. This is followed by the dyes Pyridine 1, IR 140 and IR 26 which have relatively less efficiency of diffraction at 532 nm. For CV, the signal was found to be sensitive to the large number of laser shots due to bleaching effect.

#### 5. Conclusions

The diffraction efficiency of transient gratings of laser dyes has been measured by ps laser excitation. Theoretical calculations of diffraction efficiency and  $\chi^{(3)}$  are also given here for RB.  $\chi^{(3)}$  for R6G has been measured as a function of the refractive index. Orientational relaxation times have been obtained by using degenerate four wave mixing.

#### Acknowledgments

We thank DST, New Delhi for financial assistance. This work was in part supported by a grant-in-aid No. 03 (0957)/02/EMR-II from CSIR, New Delhi.

#### References

- [1] H J Eichler, P Gunter and D W Pohl *Laser Induced Transient Grating* (Berlin : Springer-Verlag) (1986)
- [2] N Wiese, H J Eichler and J Salk *IEEE J. Quantum Electron.* 25 403 (1989)
- [3] D Langhans, J Salk and N Weise *Physica* 144C 411 (1987)
- [4] P B Bisht *Rev. Chem. Intermed.* 27 539 (2001)
- [5] R J Rajesh and P B Bisht *Chem. Phys. Lett.* 357 420 (2002)
- [6] R S Moog, M D Ediger, S G Boxer and M D Fayer *J. Phys. Chem.* 86 4694 (1982)
- [7] E Vauthey and A Henseler *J. Phys. Chem.* 99 8652 (1995)

- [8] J-C Gomy, O Nicolet and E Vauthey *J. Phys. Chem.* **A103** 10737 (1999)
- [9] E Vauthey *J. Phys. Chem.* **A105** 340 (2001)
- [10] M Terazima in *Advances in Photochem.* Vol. **24** (eds) D C Neckers, D H Volman and G von Bunau (New York . John Wiley) (1998)
- [11] J D Jackson *Classical Electrodynamics* (Wiley Eastern) (1975)
- [12] H Kogelnik *Bell System Tech. J.* **48** 2909 (1969)
- [13] M Sandrai and G R Bird *Opt. Commun.* **51** 62 (1984)
- [14] F W D Deeg and M D Fayer *J. Chem. Phys.* **91** 2269 (1989)
- [15] A B Myers and R M Hochstrasser *IEEE J. Quantum Electron.* **22** 1482 (1986)
- [16] J R Salcedo, A E Siegman, D D Dlott and M D Fayer *Phys. Rev. Lett.* **41** 131 (1978)
- [17] H J Eichler, D Langhans and F Massman *Opt. Commun.* **50** 117 (1984)
- [18] R J Rajesh, T S Natarajan and P B Bisht *Indian J. Pure Appl. Phys.* **39** 636 (2001)
- [19] R J Rajesh, P B Bisht and B M Sivaram *Int. Conf. on Math. Modeling of Nonlinear Systems* (Kharagpur : IIT) p 134 (1999)
- [20] P Hammond *IEEE J. Quantum Electron.* **15** 624 (1979)
- [21] D W Phillon, D J Kuizenga and A E Siegman *Appl. Phys. Lett.* **27** 85 (1975)
- [22] J R Lakowicz *Principles of Fluorescence Spectroscopy* (New York : Plenum) (1983)
- [23] Mini Jose *M.Sc. Thesis* (IIT Madras, India) (2002)
- [24] G R Fleming *Chemical Applications of Ultrafast Spectroscopy* (New York . Oxford Univ. Press) (1996)